Periodic vortex and current structures in superconductor-ferromagnet bilayer

G. M. Maksimova,[1] R. M. Ainbinder,[1] and D. Yu. Vodolazov[1,2]
[1]*Department of Theoretical Physics, Nizhny Novgorod University, 23 Gagarin Avenue, 603600 Nizhny Novgorod, Russia*
[2]*Institute for Physics of Microstructures, Russian Academy of Sciences, GSP-105, 603950 Nizhny Novgorod, Russia*
(Received 29 February 2008; revised manuscript received 8 September 2008; published 4 December 2008)

The formation of a periodic vortex and current structures in the ferromagnet/superconductor bilayer with finite interlayer distance a is considered when the ferromagnetic film has a stripe domain structure with out-of-plane magnetization. The integrodifferential equation which determines the current and vortex distribution in the superconducting (SC) film is derived. The analytical solutions are obtained for two limiting cases: $L<\lambda$ (the narrow-domain structure) and $L\gg\lambda$ (the wide-domain structure), where L is the width of the domain and $\lambda=\frac{\lambda_L^2}{d_s}$ is the effective penetration depth (where λ_L is the London penetration depth and d_s is the thickness of the SC film). The conditions for existence of two periodic vortex structures in the SC are found (i) for the chains of vortices/antivortices (one vortex/antivortex per domain) and (ii) for the domelike vortex distribution characterized by the average vortex density $n(x)$. The value of the critical current (along the domains) of the superconducting film is calculated. It is shown that there is the optimal interlayer distance a^* corresponding to the maximal value of the critical current at a given value of the magnetization.

DOI: 10.1103/PhysRevB.78.224505 PACS number(s): 74.25.Op, 74.25.Qt, 74.25.Sv, 75.60.−d

I. INTRODUCTION

Over the past few years a hybrid superconductor/ferromagnet (SC-FM) system has attracted considerable interest. If the proximity effect is suppressed by the oxide layer between the SC and FM components, they interact via magnetic field (for a review, see Ref. 1). This interaction results in many interesting phenomena, even if the SC and FM are not electrically coupled. The examples of such phenomena are the pinning of vortices by small magnetic particles,[2,3] spontaneous creation of a vortex-antivortex pair by the FM,[4–7] formation of a vortex-antivortex lattice in a thin superconducting film, covered with a lattice of out-of-plane magnetic dots,[8] magnetic-field-induced superconductivity,[9] and many others.

A lot of attention has recently been paid to superconductor ferromagnet bilayers (SFBs).[10–15] In Ref. 11 it was studied that the equilibrium structure of SFB is formed by a thin ferromagnet film with a perpendicular magnetic anisotropy and a thin superconducting film. It was shown that the SFB split into domains in which both the magnetization and the vortex density alternate. Also the average vortex density n was determined when the domain linear size L was much greater than the effective penetration depth $\lambda=\frac{\lambda_L^2}{d_s}$. Here λ_L is the London penetration depth and d_s is the thickness of the SC film: $d_s\ll\lambda_L$. It was found that the density $n_v(x)$ has a strong singularity near the domain walls. Erdin *et al.*[11] assumed that this is due to the fact that the using approximation becomes invalid in a region of width λ near the domain walls. However as would be shown in the present paper the perpendicular component of the magnetic field produced by the FM and the sheet current density in the Meissner state of SFB with narrow-domain structure ($L\ll\lambda$) diverge at the domain walls as well.

To avoid any singularities we analyze in this work the formation of a periodic vortex structure in the composite system, consisting of thin FM and SC films separated by finite distance a (Fig. 1). This parameter, just as the magnetization, determines the strength of interaction between the vortex and FM film.

The paper is organized as follows. In the Sec. II the integrodifferential equation for the current density in the SC film is derived. The analytical solution of the equation for the Meissner current density is found for two limiting cases: $L<\lambda$ and $L\gg\lambda$. This solution is used in Sec. III to study the total energy of the chain of the vortices with alternating directions coinciding with the direction of the magnetization in the ferromagnetic domain. The question of stability of such vortex configuration is then analyzed. The mixed state of the SC/FM heterostructure with many vortices per domain is considered in Sec. III. In Sec. IV we study the influence of the domain structure of the FM on the critical current of the superconducting film (and conclusions are given in Sec. IV).

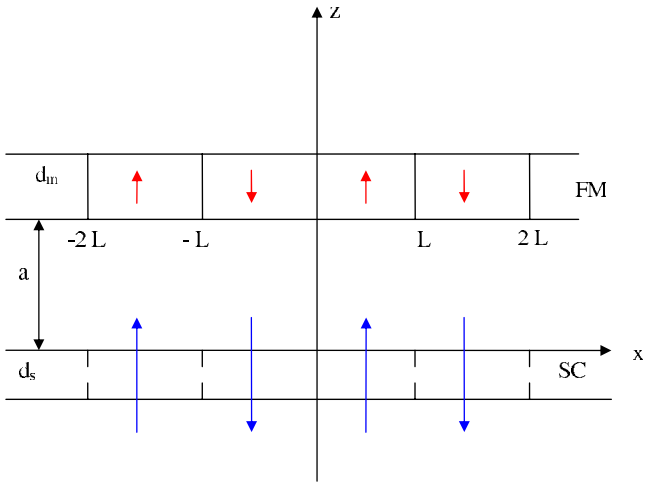

FIG. 1. (Color online) Geometry of the system consisting of the uniaxial ferromagnetic film located at distance a above thin superconducting film ($d_m\ll\lambda$, $d_s\ll\lambda$). The magnetization vectors in the domains are shown by the gray arrows. The blue arrows indicate the vortices of different polarities located in the superconducting film.

II. BASIC EQUATION

The ferromagnet-superconductor system under our consideration is shown in Fig. 1. Let the easy magnetization axis be parallel to the z axis. We assume that the ferromagnet has the domain structure formed by strips of a fixed width L parallel to the y axis. At the condition $\delta \ll L$ (where δ is the domain-wall thickness) a good approximation of the magnetization is a steplike function along the x axis. The Fourier expansion of this function at $d_m \to 0$ is

$$\vec{M} = m\vec{e}_z \delta(z-a) \sum_{k=0} \frac{4 \sin \frac{\pi(2k+1)x}{L}}{\pi(2k+1)}.$$

As it follows from this expression, the magnetic current $\vec{j}^{\mathrm{FM}} = c \,\mathrm{rot}\, \vec{M}$ has only one component $j_y^{\mathrm{FM}}(x,z)$ so that the vector potential $\vec{A}^{\mathrm{FM}}(x,z)$ generated by the FM is also directed along the y axis and can be obtained from the Maxwell equation,

$$\mathrm{rot}\ \mathrm{rot}\ \vec{A}^{\mathrm{FM}} = \frac{4\pi}{c}\vec{j}^{\mathrm{FM}},$$

$$A_y^{\mathrm{FM}}(x,z) = -2m \ln \frac{\cosh \frac{\pi(z-a)}{L} + \cos \frac{\pi x}{L}}{\cosh \frac{\pi(z-a)}{L} - \cos \frac{\pi x}{L}}. \quad (1)$$

According to Eq. (1) the magnetic field $\vec{H} = \mathrm{rot}\, \vec{A}^{\mathrm{FM}}$ has two components: $H_z(x,z)$ and $H_x(x,z)$. Specifically, the perpendicular component of the field at the SC film ($z=0$) is given by the expression

$$H_z(x,z=0) = \frac{4\pi m \cosh \frac{\pi a}{L}}{L} \frac{\sin \frac{\pi x}{L}}{\sin^2 \frac{\pi x}{L} + \sinh^2 \frac{\pi a}{L}}. \quad (2)$$

Depending on the distance a between the FM and SC the maximum value of $H_z(x,z=0)$ may be reached either near the domain walls (at $a < a_0$, where $a_0 = \frac{L}{\pi}\,\mathrm{arcsinh}\ 1$) or at the center of the domain ($a > a_0$) (Fig. 2).

As was mentioned in Sec. I, the thickness of the superconducting film is $d_s \ll \lambda_L$. Suppose that its width $w(-\frac{w}{2} \le x \le \frac{w}{2})$ and length $b(-\frac{b}{2} \le y \le \frac{b}{2})$ satisfy the conditions $\max(L,\lambda) \ll w \ll b$. In the presence of the SC and FM films the vector-potential $\vec{A}$ (in the gauge $\mathrm{div}\, \vec{A} = 0$) satisfies the equation

$$\Delta \vec{A} = -\frac{4\pi}{c}(\vec{j}^{\mathrm{FM}} + \vec{j}), \quad (3)$$

where $\vec{j}$ is the current density induced in the superconducting film by the magnetic field of the ferromagnet. Since the vector potential of the field $\vec{A}^{\mathrm{FM}}(x,z)$ is directed along the y axis, i.e., along the SC strip, we can conclude that both $\vec{j}$ and $\vec{A}(x,z)$ are along the y direction also, as in the case of the SC strip placed into uniform perpendicular magnetic field.[16–18] In the thin-film approximation, the current density $j_y(x,z)$ is averaged over the thickness of the SC film. The average current density is denoted by $j(x)$ so that

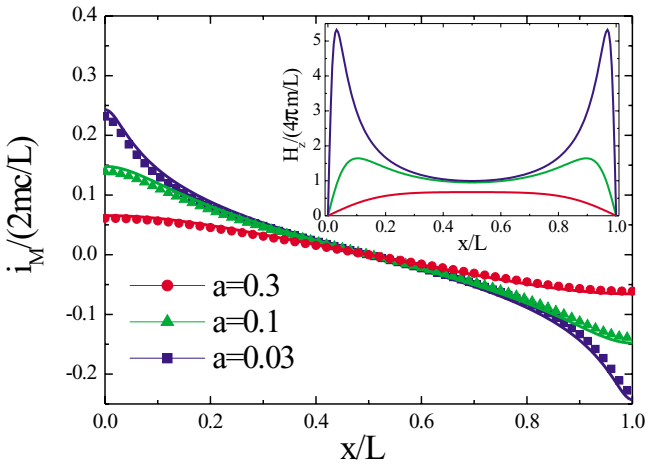

FIG. 2. (Color online) Distribution of the sheet current density $i_M(x)$ over the domain for narrow-domain structure for three values of interlayer distance a between the SC and the FM films. Solid symbols correspond to numerical solution of Eq. (10) and curves in Eq. (11). In the inset we present distribution of the magnetic field induced by the FM.

$$j_y(x,z) = d_s j(x)\delta(z)\theta\left(\frac{w^2}{4} - x^2\right) \quad (4)$$

Then, Eq. (3) is solved by introducing the Green's function for the two-dimensional Laplacian, $G(x-x',z-z')$,[17,18]

$$A_y(x,z) = A_y^{\mathrm{FM}}(x,z) - 4\pi d_s \int_{-w/2}^{w/2} G(x-x',z) j(x')dx', \quad (5)$$

where $A_y^{\mathrm{FM}}(x,z)$ is determined by Eq. (1). The current density $j(x)$ is connected with the vector potential $A_y(x,z=0) = A_y(x)$ by the known London equation

$$A_y(x) = -\frac{4\pi\lambda_L^2}{c} j(x) + \Phi_y(x), \quad (6)$$

where the last term $\Phi_y(x)$ describes (in the continuous approximation) the contribution of vortices into $A_y(x)$. Substituting Eq. (6) into Eq. (5) at $z=0$ and differentiating both sides of Eq. (5) with respect to x, we arrive at the following integrodifferential equation—the Maxwell-London equation for the sheet current density $i(x) = j_y(x)d_s$:

$$\frac{4\pi\lambda}{c}\frac{di}{dx} + \frac{2}{c}\int_{-w/2}^{w/2} \frac{i(t)dt}{t-x} = -H_z(x) + \Phi_0 n(x), \quad (7)$$

where $H_z(x)$ is the perpendicular component of the magnetic field, produced by the ferromagnet [Eq. (2)], Φ_0 is the magnetic-flux quantum, and $n(x)$ is the averaged vortex density which should also be found from this equation. When deriving Eq. (7), we use $\frac{\partial G(x-x',0)}{\partial x} = \frac{1}{2\pi(x-x')}$.

It should be noted that longitudinal component of the magnetic field H_x does not affect the solution of our problem

in thin-film geometry. Really, this field induces the Meissner current flowing in opposite directions along two surfaces of the SC film that leads to average zero value. Also, we can neglect the suppression of the order parameter by H_x because the ratio between the critical magnetic field perpendicular to film direction $H_z^c \sim \Phi_0/\xi\sqrt{w\lambda}$ (Ref. 17) and critical magnetic field parallel to film direction $H_x^c \sim \Phi_0/\xi d$ is much smaller than unity for our model system with $d/w \ll 1$ and $d/\lambda_L \ll 1$. Therefore Eq. (7) is valid until the parallel component of the magnetic field becomes comparable with H_x^c.

Due to the symmetry of the problem the sheet current density satisfies the equation $i(t-n\,L)=(-1)^n i(t)$ and the second term at the left-hand side of Eq. (4) may be represented in the form

$$\sum_{-n_{\max}}^{n_{\max}} \int_{nL}^{(n+1)L} \frac{i(t)dt}{t-x} = \sum_{-n_{\max}}^{n_{\max}} \int_0^L \frac{i(t)(-1)^n dt}{t-(x-nL)}, \tag{8}$$

where $n_{\max}=\frac{w}{2L}$.

Introducing the quantity $u=\frac{t-x}{L}$, we rewrite the sum in Eq. (8) as

$$S=\frac{1}{L}\sum_{n=-n_{\max}}^{n=n_{\max}} \frac{(-1)^n}{u+n} = \frac{1}{L}\left(\frac{1}{u}+2u\sum_{n=1}^{n=n_{\max}} \frac{(-1)^n}{u^2-n^2}\right),$$

which in the limit $n_{\max}\to\infty$ is reduced to the expression[19]

$$S=\frac{\pi}{L\sin(\pi u)}. \tag{9}$$

After that, substituting Eq. (9) into Eq. (7) we arrive at the following integrodifferential equation for the current density:

$$\frac{4\pi\lambda}{c}\frac{di}{dx}+\frac{2\pi}{cL}\int_0^L \frac{i(t)dt}{\sin\frac{\pi(t-x)}{L}} = -H_z(x)+\Phi_0 n(x). \tag{10}$$

First we consider the Meissner state of the superconducting film $[n(x)=0]$. The solution of Eq. (10) for Meissner current density $i_M(x)$ depends on two parameters: λ/L and a/L. For enough thin SC films the effective penetration depth λ may be much larger than the domain size: $\lambda \gg L$. For such narrow-domain SC-FM structure the self-field of the current [the second term in Eq. (10)] may be neglected. After that, using the expression for $H_z(x)$ [Eq. (2)] we find from Eq. (10)

$$i_M(x)=\frac{cm}{2\pi\lambda}\ln\frac{\cosh\frac{\pi a}{L}+\cos\frac{\pi x}{L}}{\cosh\frac{\pi a}{L}-\cos\frac{\pi x}{L}}. \tag{11}$$

As it follows from Eq. (11) at the domain walls the value of the Meissner current density is maximal

$$|i_M(x=nL)|=\frac{cm}{\pi\lambda}\ln\coth\frac{\pi a}{2L}. \tag{12}$$

In Fig. 2 we present the result of the numerical solution of Eq. (10) $[n(x)=0]$ and sheet-current density $i_M(x)$ calculated from Eq. (11) for $\lambda \geq L$ and the different values of the parameter a/L. As can be seen in the figure the analytical profiles clearly agree with the numerical ones right until $\lambda \sim L$.

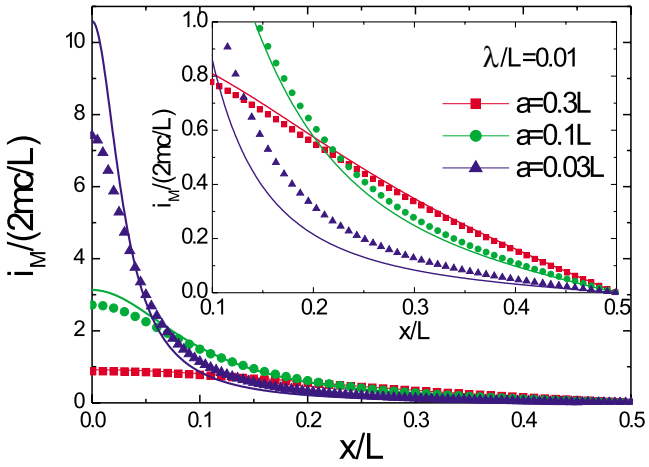

FIG. 3. (Color online) Distribution of sheet current density $i_M(x)$ over the half of domain for wide-domain structure for three values of interlayer distance a between the SC and the FM films. Solid symbols correspond to numerical solution of Eq. (10) and curves in Eq. (17). In the inset we present the zoom of current distribution far from domain boundary.

In the opposite case $\lambda \ll L$ and for $a \gg \lambda$ the first term in Eq. (10) is much smaller than the second almost everywhere inside the domains except in a region of a width λ near the domain wall. By using the obvious symmetry $i(x)=-i(L-x)$ and introducing the following transformation of the variable,

$$z=\sin^2\frac{\pi x}{L}, \quad \frac{L}{2}\leq x \leq L. \tag{13}$$

Equation (10) is reduced to the well-known singular equation of the Cauchy type for $i(u)/\sqrt{u}$,

$$\frac{2}{c}\int_0^1 \frac{i(u)du}{\sqrt{u}(u-z)} = \frac{H_0}{z+\gamma^2}-\frac{\Phi_0 n(z)}{\sqrt{z}}, \tag{14}$$

where

$$H_0=\frac{4\pi m}{L}\sqrt{1+\gamma^2}, \quad \gamma=\sinh\frac{\pi a}{L}. \tag{15}$$

The current distribution obtained from Eq. (14) in the Meissner state $[n(z)=0]$ is expressed as

$$i_M(z)=-\frac{cH_0\gamma}{2\pi\sqrt{1+\gamma^2}}\frac{\sqrt{1-z}}{z+\gamma^2}, \tag{16}$$

or in the original variables $(0\leq x\leq L)$,

$$i_M(x)=\frac{2cm\gamma}{L}\frac{\cos\frac{\pi x}{L}}{\sin^2\frac{\pi x}{L}+\gamma^2}. \tag{17}$$

Figure 3 shows $i_M(x)$ obtained from Eq. (17) for $\frac{\lambda}{L}=0.01$ several values of the distance a between the SC and FM films. For comparison the numerical solution of Eq. (10) is

also shown. It can be seen that the analytical results [Eq. (17)] are in good agreement with the numerical calculations if the separation a is larger than λ. At small $a \leq \lambda$ the magnetic field of the FM $H_z(x)$ [see Eq. (2)] is strongly changed near the domain wall that leads to an increase in the differential term in Eq. (10). So in this case Eq. (14) and its solution for $i_M(x)$ [Eqs. (16) and (17)] become invalid. We assume in this paper that if $\lambda \ll L$ then $a \gg \lambda$.

III. CHAIN OF VORTICES INSIDE THE SUPERCONDUCTING STRIP

When the maximum current density reaches the value $i_M = j_{dep} d_s$ (where j_{dep} is the depairing current density)[20,21] vortices can penetrate into a superconducting layer near the domain wall. Here we consider the simple realization of such vortex state: the chain of vortices (along the x axis) with alternating directions corresponding to the direction of the magnetization in the ferromagnetic domains (Fig. 1).

The total energy of such a chain per domain is the sum of two terms,

$$E(x_0) = E_s(x_0) + E_{v-f}(x_0). \tag{18}$$

The first one is the energy of the vortex located at $x = x_0 (0 < x_0 < L)$, including its interaction with other vortices. For the narrow-domain structure ($L \ll \lambda$) $E_s(x_0)$ coincides with the energy of a vortex inside thin narrow SC film,[22]

$$E_s(x_0, L \ll \lambda) = \varepsilon_0 \ln\left[\frac{L}{\pi\xi}\sin\left(\frac{\pi x_0}{L}\right)\right], \quad \xi \leq x_0 \leq L - \xi, \tag{19}$$

where ξ is the coherence length, $\varepsilon_0 = \frac{\Phi_0^2}{16\pi^2\lambda}$, and Φ_0 is the magnetic-flux quantum.

In the opposite case when the domain size L is much greater than the characteristic length of the vortex interaction λ, the single-vortex energy $E_s(x_0)$ is the same as the energy of one vortex located in infinite SC film,

$$E_s(x_0, L \gg \lambda) = \varepsilon_0 \ln\left(\frac{2\lambda}{\xi}\right). \tag{20}$$

Equation (20) holds (in lowest order in $\frac{\lambda}{L}$) for all $0 < x_0 < L$ except within a narrow region of width λ near the domain boundaries. If $\xi < x_0 \ll \lambda$ the interaction with the vortex located at $x = -x_0$ in the neighboring domain becomes essential so that

$$E_s(\xi < x_0 \ll \lambda, L \gg \lambda) = \varepsilon_0 \ln\left(\frac{2x_0}{\xi}\right). \tag{21}$$

The second term in Eq. (18) corresponds to the interaction energy between the vortex and magnetic structure,[23,24] which may be represented as the energy of a vortex interacting with the Meissner current,[7]

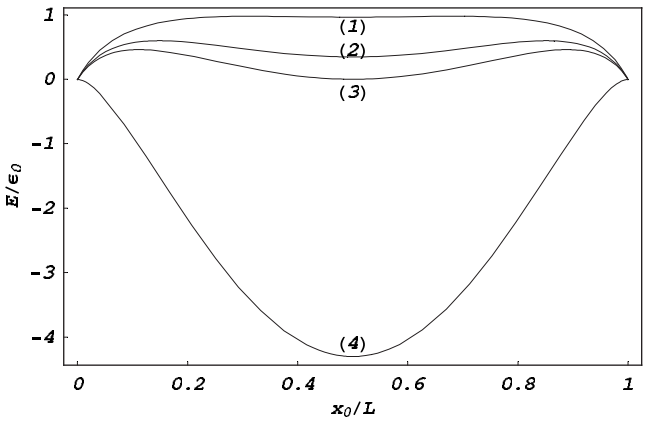

FIG. 4. Normalized total energy of the vortex interacting with the FM strip and other vortices as a function of its position for different magnetizations: (1) $\frac{m}{m_0} = 11.8$, (2) $\frac{m}{m_0} = 19$, (3) $\frac{m_c}{m_0} = 23$, and (4) $\frac{m_s}{m_0} = 73$. Here $m_0 = \frac{\Phi_0}{4\pi\lambda}$, $\frac{L}{\lambda} = \frac{1}{2}$, $\frac{a}{L} = \frac{2}{\pi}$, and $\frac{\xi}{L} = \frac{0.16}{\pi}$.

$$E_{v-f}(x_0) = -\frac{\Phi_0}{2c}\int_0^{x_0} i(x)dx, \tag{22}$$

where the current density $i(x) = i_M(x)$ is determined by Eqs. (11) and (17) for $L < \lambda$ and $L \gg \lambda$, respectively. Figure 4 shows the normalized energy of vortex chain (per vortex) obtained from Eqs. (11), (18), (19), and (22) for different values of the magnetization M.

At the equilibrium all vortices are located at the centers of their domains due to the symmetry. If the vortex energy $E(x_0 = L/2) > 0$ then the considering configuration of the vortices is metastable. The minimum vortex energy $E(x_0 = L/2)$ becomes negative if $m > m_c(a)$, where

$$m_c(a) = \frac{\Phi_0}{4\pi L}\frac{\ln\frac{L}{\pi\xi}}{\int_0^{1/2}\ln\frac{\cosh\frac{\pi a}{L} + \cos\pi t}{\cosh\frac{\pi a}{L} - \cos\pi t}dt} \quad \text{for } L < \lambda \tag{23}$$

and

$$m_c(a) = \frac{\Phi_0}{16\pi\lambda}\frac{\ln\frac{\lambda}{\xi}}{\arctan\left(1/\sinh\frac{\pi a}{L}\right)} \quad \text{for } L \gg \lambda. \tag{24}$$

It is clear that if the FM strip is displaced higher above the SC film, the interaction becomes weaker and it is necessary to increase the value m_c to satisfy the condition $E(x_0 = L/2) = 0$. The minimum value $m_c^{\min}$ for the narrow-domain structure $L < \lambda$ is determined from Eq. (20) at $a = 0$: $m_c^{\min} = \frac{\Phi_0}{16LG}\ln\frac{L}{\pi\xi}$, $L < \lambda$, where $G \approx 0.916$ is the Catalan constant. For the wide-domain structure at $\lambda < a \ll L$ $m_c(a)$, as it follows from Eq. (24), weakly depends on the distance a and equals

$$m_c = \frac{\Phi_0}{8\pi^2\lambda}\ln\frac{\lambda}{\xi}. \tag{25}$$

The energy minimum at $x_0=L/2$ is separated from the domain boundaries by the energy barrier (annihilation barrier) which prevents the creation of the vortex-antivortex pairs and penetration of the vortices into the domains. The height of this barrier decreases by an increase in the magnetization M, and at some value $m=m_s(a)>m_c(a)$ the barrier is suppressed. The critical magnetization $m_s(a)$ determines the transition to the mixed state. From the condition

$$\left.\frac{\partial E(x_0)}{\partial x_0}\right|_{x_0=\xi} = 0, \tag{26}$$

we find

$$m_s(a) = \frac{\Phi_0}{8\pi\xi}\frac{1}{\ln\coth\dfrac{\pi a}{2L}}, \quad L<\lambda, \tag{27a}$$

$$m_s(a) = \frac{\Phi_0 L \sinh\dfrac{\pi a}{L}}{16\pi^2\lambda\xi}, \quad \lambda \ll L. \tag{27b}$$

For magnetization $m<m_c(a)$ the vortex-ferromagnet interaction reduces, which leads to the positive value of the vortex energy at the local minimum $E(x_0=L/2)>0$ (Fig. 5). At $m<m_1(a)$ this minimum disappears and vortices and antivortices tend to leave off their domains and annihilate near the domain boundaries. Thus $m_1(a)$ determines the lower boundary of the metastable states of vortex chain in the superconducting film. The value $m_1(a)$ may be found from the equation

$$\left.\frac{\partial^2 E}{\partial x_0^2}\right|_{x_0=L/2} = 0. \tag{28}$$

Using this condition and Eqs. (11), (18), (19), and (22) we obtain for the narrow-domain structure

$$m_1(a) = \frac{\Phi_0}{8L}\cosh\frac{\pi a}{L}, \quad L<\lambda. \tag{29}$$

To calculate the corresponding value for the wide-domain structure we need a more accurate expression than Eq. (20) for the energy of vortex inside the domain ($x_0 \gg \lambda$), including its interaction with vortices located in the neighborhood. This expression is found in the Appendix. Using Eqs. (17), (18), (22), and (A4) we have

$$m_1(a) = \frac{2\Phi_0}{\pi^3 L}\left(\gamma+\frac{1}{\gamma}\right), \quad \lambda \ll L. \tag{30}$$

Notice that our results for considering here the vortex structure with one vortex per domain may be applied also for configurations with one chain of vortices per domain if the vortex-vortex distance is large enough (at least larger than λ). Earlier Erdin *et al.*[15] considered the discrete lattice of vortices (in SFB with zero distance between ferromagnet and superconductor) in which the vortices are situated periodically on chains in the stripe domains. From his numerical calculations it follows that if the FM domain size is fixed, the configurations with a single-vortex chain per domain appear first in the mixed state that correlates with our results.

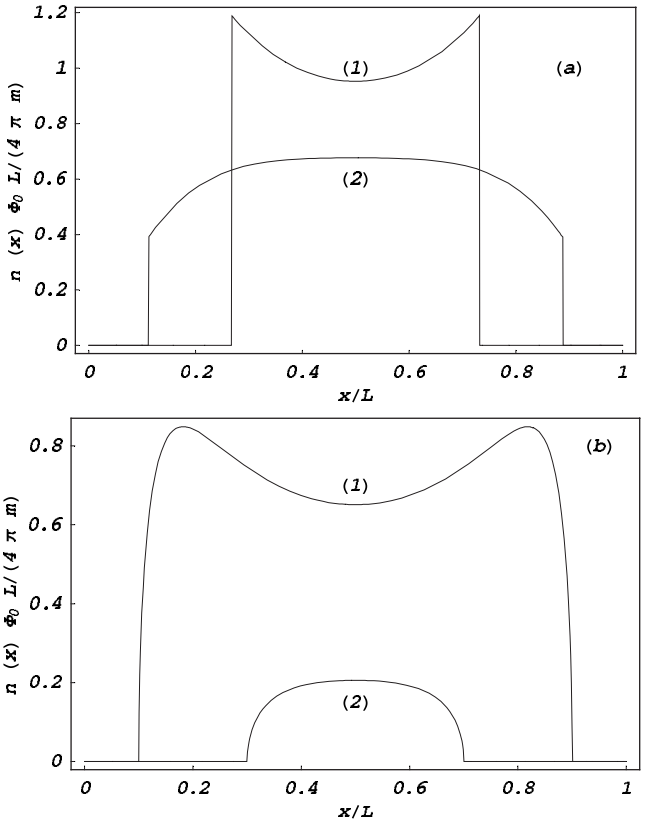

FIG. 5. (a) The vortex density in narrow-domain structure for various values of the separation a between the films: (1) $\frac{a}{L}=0.1$ and (2) $\frac{a}{L}=0.3$. (b) The vortex density in wide-domain structure for various values of the separation a between the films: (1) $\frac{a}{L}=0.1$ and (2) $\frac{a}{L}=0.3$.

IV. MIXED STATE OF THE SC/FM BILAYER

Now we consider the vortex structure of the SC/FM bilayers with many vortices per domain which is characterized by the average density $n(x)$. In the absence of a bulk pinning this function is nonzero in the region of the SC film where the sheet current density $i(x)=0$. This condition allows us to find $n(x)$ and $i(x)$ from Eq. (10).

A. Narrow-domain structure

In the leading approximation with respect to $L/\lambda \ll 1$, from Eq. (10) we obtain inside the domain $0 \le x \le L$,

$$n(x) = \begin{cases} 0, & x \le \Delta \\ \dfrac{H_z(x)}{\Phi_0}, & \Delta \le x \le L-\Delta \\ 0, & L-\Delta \le x \le L, \end{cases} \tag{31}$$

$$i(x) = \begin{cases} i_M(x) - i_M(\Delta), & 0 \le x \le \Delta \\ 0, & \Delta \le x \le L - \Delta \\ i_M(x) + i_M(\Delta), & L - \Delta \le x \le L, \end{cases} \tag{32}$$

where $H_z(x)$ and $i_M(x)$ are determined by Eqs. (2) and (11). The trapped flux Φ inside a domain (per unit length) corresponding to this distribution of vortices is

$$\Phi(\Delta) = \Phi_0 \int_{\Delta}^{L-\Delta} n(x)dx = 4m \ln \frac{\cosh\frac{\pi a}{L} + \cos\frac{\pi\Delta}{L}}{\cosh\frac{\pi a}{L} - \cos\frac{\pi\Delta}{L}}, \tag{33}$$

where Δ is a parameter, characterizing the width of the region l occupied by the vortices; $l=L-2\Delta$.

Figures 5(a) and 5(b) show the vortex density (at given value of Φ) for various values of the separation a between the films correspondingly. Note that as it follows from Eqs. (2) and (31) at $a > a_0$, where $a_0 = \frac{L}{\pi}$ arcsinh 1 a domelike flux distribution appears [see curve 2 in Fig. 5(a)].

The mixed state described by Eqs. (31)–(33) is stable (more precisely, metastable) as long as there are energy barriers for vortex entry in each domain and vortex exit from it. To find the boundaries of the region for the existence of such metastable mixed states with the fixed trapped flux Φ, we assume that there is one test vortice (with corresponding polarity) in each domain. Such vortices placed periodically in the SC film form the vortex chain along the x axis. The energy of the test vortex $E(x_0,\Phi)$ placed in the vortex-free region $\xi \le x_0 \le \Delta(\Phi)$ is obtained from Eqs. (18), (19), and (22), but unlike in Sec. III the current density $i(x)$ in Eq. (22) is determined by Eq. (32);

$$E(x_0,\Phi) = \frac{\Phi_0^2}{16\pi^2\lambda} \ln\left(\frac{L}{\pi\xi}\sin\frac{\pi x_0}{L}\right) + \frac{\Phi\Phi_0 x_0}{16\pi\lambda} - \frac{m\Phi_0}{4\pi\lambda}\int_0^{x_0} \ln\frac{\cosh\frac{\pi a}{L} + \cos\frac{\pi x}{L}}{\cosh\frac{\pi a}{L} - \cos\frac{\pi x}{L}}dx. \tag{34}$$

The magnetization $m_{en}(\Phi)$, at which the barrier for vortex entry is suppressed and vortice pairs of different polarity nucleates at the domain wall, can be found from Eqs. (26) and (34),

$$m_{en}(\Phi) = m_s + \frac{\Phi}{8 \ln \coth\frac{\pi a}{2L}}, \tag{35}$$

where m_s is the magnetization for entry of the first vortex [Eq. (27a)] into the domain. At low magnetization $m \le m_{ex}(\Phi)$ the dependence $E(x_0,\Phi)$ on x_0 becomes monotonic that corresponds to disappearance of the barrier to vortex exit from the domain. So $m_{ex}(\Phi)$ may be found from the conditions

$$\frac{\partial E(x_0,\Phi)}{\partial x_0} = 0, \quad \frac{\partial^2 E(x_0,\Phi)}{\partial x_0^2} = 0. \tag{36}$$

Substituting Eq. (34) into Eq. (36) we arrive at the following equations for x_0 and $m=m_{ex}(\Phi)$:

$$\frac{\Phi_0}{L}\cot\frac{\pi x_0}{L} + \Phi = 4m \ln\frac{\cosh\frac{\pi a}{L} + \cos\frac{\pi x_0}{L}}{\cosh\frac{\pi a}{L} - \cos\frac{\pi x_0}{L}}, \tag{37a}$$

$$\frac{\Phi_0}{L} = \frac{8m\cosh\frac{\pi a}{L}\sin^3\frac{\pi x_0}{L}}{\cosh^2\frac{\pi a}{L} - \cos^2\frac{\pi x_0}{L}}. \tag{37b}$$

In the range of values of m near $m_1(a)$, as it follows from Eqs. (37a) and (37b),

$$m_{ex}(\Phi) = m_1(a)\left\{1 + \frac{3}{2}\left[\frac{L}{\Phi_0}\left(1 - \frac{2}{3\cosh^2 \pi a/L}\right)^{1/2}\Phi\right]^{2/3}\right\}, \tag{38}$$

where $m_1(a)$, the lower stability boundary of the vortex chain, is determined by Eq. (29). Note that such dependence $m_{ex}(\Phi)$ at small values of the flux Φ is similar to the dependence of the exit magnetic field $H_{ex}(\Phi)$ for narrow SC strip exposited in the perpendicular magnetic field.[22] For $m \gg m_1(a)$,

$$m_{ex}(\Phi) = \frac{\Phi}{2 \ln \coth\frac{\pi a}{2L}}. \tag{39}$$

B. Wide-domain structure

We now turn to the solution of Eq. (10) for small λ/L. As it was shown in Sec. II in this case (and for $a > \lambda$) the first term in Eq. (10) can be dropped and current and vortex distributions can be found from integral (14). When the current density at the edges of the domain becomes equal to the depairing current density, vortices nucleate at the domain's edges and penetrate into the domain occupying the central region $\delta \le x \le L-\delta$. The resulting current flows in the vortex-free region of width x_0 near the edges of the domain and satisfies the equation

$$\frac{2}{c}\int_0^{u_0} \frac{i(u)du}{\sqrt{u}(u-z)} = \frac{H_0}{z+\gamma^2}, \tag{40}$$

where $0 \le z \le u_0$, $u_0 = \sin^2\frac{\pi\delta}{L}$. Thus the current distribution is similar to the current density in the Meissner state [Eq. (16)],

$$i(z) = -\frac{cH_0\gamma}{2\pi\sqrt{u_0+\gamma^2}}\frac{\sqrt{u_0-z}}{z+\gamma^2}. \tag{41}$$

Returning to the original coordinates, we obtain

$$i(x) = \pm \frac{2cm\gamma}{L}\sqrt{\frac{1+\gamma^2}{u_0+\gamma^2}}\frac{\sqrt{u_0 - \sin^2\frac{\pi x}{L}}}{\gamma^2 + \sin^2\frac{\pi x}{L}}, \qquad (42)$$

where the positive (negative) sign applies to $0 \le x \le \delta (L-\delta \le x \le L)$. The corresponding density of vortex is obtained from Eq. (7) by using Eq. (41),

$$n(z) = \frac{H_0\gamma}{\Phi_0}\frac{\sqrt{z-u_0}}{\sqrt{u_0+\gamma^2}(z+\gamma^2)}, \quad u_0 \le z \le 1 \qquad (43)$$

or in the original variables ($\delta \le x \le L-\delta$),

$$n(x) = \frac{4\pi m\gamma}{\Phi_0 L}\sqrt{\frac{1+\gamma^2}{u_0+\gamma^2}}\frac{\sqrt{\sin^2\frac{\pi x}{L} - u_0}}{\gamma^2 + \sin^2\frac{\pi x}{L}}. \qquad (44)$$

Equation (44) shows that the vortex density has a dome-like distribution within the domain if the boundary of the vortex-filled region δ satisfies the condition

$$\cos\frac{2\pi\delta}{L} \le \sinh^2\frac{\pi a}{L}. \qquad (45)$$

Obviously, this inequality holds for any values of the distance a between the FM and SC films if the trapped vortex flux is low enough that $\delta > \frac{L}{4}$. For sufficiently large a, $\sinh\frac{\pi a}{L} > 1$ and any values of δ inequality (45) holds, also. Figure 7 shows the vortex distribution for various values of parameter a and δ.

By means of standard integration one finds the magnetic flux connected with the vortex structure

$$\Phi = \Phi_0\int_{\delta}^{L-\delta} n(x)dx = 8\gamma m\varphi(q), \qquad (46)$$

$$\varphi(q) = \frac{K(q) - (1-n)\Pi(n,q)}{\sqrt{1-n}}. \qquad (47)$$

Here $q = \sqrt{1-u_0} = \cos\frac{\pi\delta}{L}$, $n = \frac{q^2}{1+\gamma^2} = \frac{\cos^2\pi\delta/L}{\cosh^2\pi a/L}$, $K(q)$, and $\Pi(n,q)$ are complete elliptic integrals of the first and third kinds, respectively. For $a \ll L$, $n \approx q^2$, and after some algebra we obtain from Eqs. (46) and (47)

$$\Phi = \frac{8\pi am}{L}\frac{K(q) - E(q)}{\sqrt{1-q^2}}, \qquad (48)$$

where $E(q)$ is a complete elliptic integral of the second kind.

Using Eq. (39) for the current density one can compute, as in Secs. I–III, the critical magnetizations, determining the boundaries of metastability of the mixed state with the fixed flux Φ. Thus the critical magnetization $m_{en}(\Phi)$ for which the annihilation barrier disappears and the next vortex penetrates into the domain can be found from the equation

$$m_s = m_{en}\sqrt{\frac{1-q^2}{1-n}}, \qquad (49)$$

where m_s is the entry magnetization for the first vortices entering the domain [Eq. (27b)].

A combination of Eqs. (43) and (46) yields the resulting equation for $m_{en}(\Phi)$,

$$\Phi = 8\gamma m_{en}\varphi\left\{\left[\left(1-\left(\frac{m_s}{m_{en}}\right)^2\right)\Big/\left(1-\left(\frac{m_s}{m_{en}}\right)^2\frac{1}{1+\gamma^2}\right)\right]^{1/2}\right\}. \qquad (50)$$

For small fluxes $\Phi \ll m_s$ the behavior of $m_{en}(\Phi)$ is characterized by the linear equation

$$m_{en}(\Phi) = m_s + \frac{\Phi\gamma}{4\pi}. \qquad (51)$$

For $\Phi \gg m_s$ vortices occupy almost all the domains. In this case. as it follows from Eqs. (2) and (44), $n(x) \approx \frac{H_z(x)}{\Phi_0}$ corresponds to the linear dependence

$$m_{en}(\Phi) = \frac{\Phi}{4\ln\frac{\sqrt{1+\gamma^2}+1}{\sqrt{1+\gamma^2}-1}}. \qquad (52)$$

A similar asymptotic solution has been obtained in Ref. 25 for the barrier-suppressing field $H_{en}(\Phi)$ for a thin-film strip of width $w (w \gg \lambda)$ placed in a perpendicular magnetic field.

V. TRANSPORT PROPERTIES OF THE SC/FM BILAYER

In this section we study the influence of the domain structure of the FM on the critical current of the superconducting film. We consider here the case when the current flows along the domains, neglects the influence of the bulk pinning, and supposes that our superconducting film is very wide $W \gg \lambda$; and the transport current is mainly concentrated near the edges of the film. As a result the sheet current density is equal to zero in the central regions of the film because $i \sim I_c/W \sim \sqrt{\lambda/W}$ with $I_c \sim \sqrt{\lambda W}$.[26,27]

When the magnetization is small or the interlayer distance a is large, the magnet-induced current density is small everywhere in the superconducting film and vortices/antivortices can appear only by entering via edges of the superconductor. Because the induced current is positive in one part of SC inside the domain and it is negative in another part of the domain (see Fig. 2), the vortices/antivortices cannot pass the film and dissipation starts only when the current density at any point inside the domain has the same sign (see black curve in Fig. 6). It gives us the criterion for finding the critical current at relatively small magnetization or large values of a: $(i_M + i_I)|_{x=L} = 0$.

With increasing magnetization (or decreasing distance a) the total sheet current density $i_M + i_I$ may reach depairing sheet current density $j_{dep}d_s$ near the edges of the domains and vortex-antivortex pairs will be created in that regions (see green curve in Fig. 6). Nucleated vortices will reach the re-

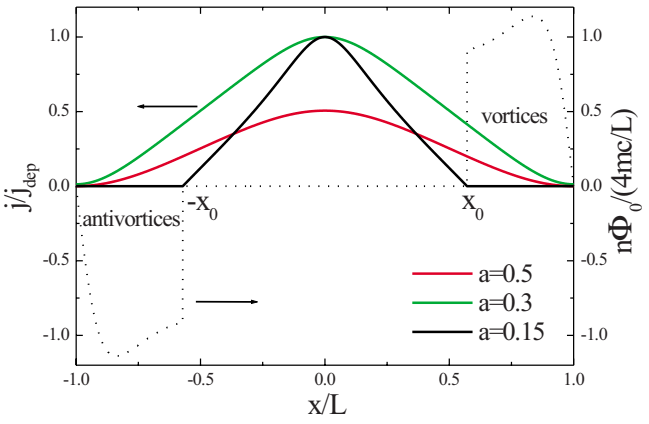

FIG. 6. (Color online) Distribution of current density $i(x)$ in two adjacent domains at $I=I_c$ for three values of interlayer distance a and $M=0.15M_0$. Dotted curved line corresponds to vortex/antivortex distribution in the superconductor at small value of a.

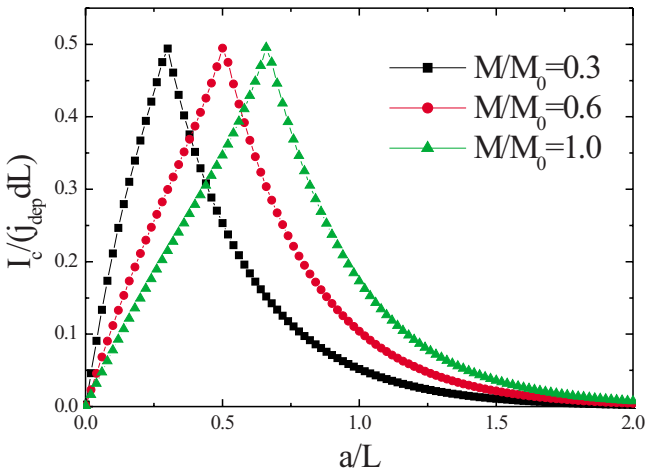

FIG. 7. (Color online) Dependence of the critical current of SC/FM bilayer on the distance between SC and FM layers for three values of magnetization M.

gion of the superconductor where the current density changes sign and stops there. In equilibrium one has $i=0$ in the region filled with vortices. The dissipation starts when the regions with vortices and antivortices touch each other under domain boundaries next to the domain boundaries where the vortices were nucleated (see Fig. 6). It gives us the criterion for finding the critical current in this range of parameters $(i_M+i_I)|_{x=0}=j_{\mathrm{dep}}d_s$. Coordinates of the region which is filled with vortices $(x_0<x<L)$ and where $i=0$ (see Fig. 6) can be found using the condition $(i_M+i_I)|_{x_0=L}=0$.

Using the above ideas we calculate the critical current (per domain) of our system as function of the distance a for different values of the magnetization. We consider the narrow domains $L\leq\lambda$ (as the more realistic case for modern FM/SC structures, see discussion below). In this limit i_I =const and using Ginzburg-Landau critical current density $j_{\mathrm{dep}}=c\Phi_0/12\sqrt{3}\pi^2\lambda_L^2\xi$ as estimation of the depairing current density $j_{\mathrm{dep}}=j_{\mathrm{GL}}$ we easily find that

$$i_{I=I_c}=\begin{cases}2j_{\mathrm{GL}}d_s\ \ln\coth(\pi a/2L)M/M_0, & a>a^*\\ j_{\mathrm{GL}}d_s(1-2\ \ln\coth(\pi a/2L)M/M_0), & a<a^*,\end{cases} \tag{53}$$

where $a^*=\frac{2L}{\pi}\arctan h(e^{-M_0/4M})$ and $M_0=\Phi_0/6\sqrt{3}\pi\xi d_m$. As a result the critical current (per domain) for our bilayer system $I_c=\int_0^L(i_M(x)+i_{I=I_c})dx$ is equal to

$$\frac{I_c}{j_{\mathrm{GL}}d_sL}=\frac{2M}{M_0}\ln\coth(\pi a/2L),\quad a>a^* \tag{54}$$

and should be calculated numerically for $a<a^*$. In Fig. 7 we present dependence $I_c(a)$ for three values of the magnetization M.

There is the optimal distance a^* when the critical current reaches the maximal value at fixed magnetization (see Fig. 7). Indeed, for small value of a the current density grows very fast near the domain boundaries and it is small in the rest of the superconductor (see Fig. 2). It results in small value of the critical current because the major part of the superconductor will be occupied by vortices and $i=0$ in that area. For large value of a the current induced by the magnet is small everywhere and the critical current is also small. We should note that at $a=a^*$ the critical current reaches half of maximal possible value $I_c^{\max}=j_{\mathrm{GL}}d_sL$ for arbitrary value of M. At $a=a^*$ and $I=I_c$ the sheet current $i(0)=j_{\mathrm{dep}}d$ and $i(L)=0$. It is obvious that for wide domains $L>\lambda$ the maximal critical current can also reach $I_c^{\max}/2$ (because in this limit the transport current density varies in the scale of the width of the film[26,27] and can be considered as constant on the scale of the domain width $L\ll W$) but the optimal distance a^* can be found only via numerical solution of Eq. (10) if $a^*<\lambda$ or by using Eq. (14) if $a^*>\lambda$.

In real superconductors the pinning current density j_p is always much smaller than the depairing (Ginzburg-Landau) current density [although the pinning mainly defines the critical current because $j_pw\gg j_{\mathrm{GL}}\lambda$ (Ref. 28) for commonly used superconductors with $w\gg\lambda$]. Therefore our results on the critical current could be applied to realistic SC/FM bilayers with interlayer distance $a\sim a^*$ when the current density is about $j_{\mathrm{GL}}/2$ almost over the whole superconductor at $I=I_c$ (see red curve in Fig. 6). The good candidate to observe the predicted effect is NbGe superconducting films [$\xi(0)\sim 7$ nm, $\lambda_L(0)\sim 1.15$ μm, and $d_s\sim 20$ nm] with its very low bulk pinning even at $T=T_c/2$ (Ref. 29) and artificial Co/Pd multilayered ferromagnetic films with out-of-plane magnetization $M\sim 300$ Oe, thickness $d_m\sim 20$ nm, and typical width of domain $L\sim 200$ nm.[30] At these parameters $L<\lambda$ (narrow domains) and $a^*\sim 3$ nm. Another good candidate is niobium superconducting thin film with $\xi(0)\sim 10$ nm, $\lambda_L(0)\sim 150$ nm, and $d_s\sim 100$ nm. For its parameters $L\sim\lambda$ and the optimal distance $a^*\sim 9$ nm is again in the range of the modern methods of fabricating SC/FM structures. For above parameters one may also neglect the influence of the current-induced magnetic field $(H_\parallel\sim j_{\mathrm{dep}}d_s/c\sim 5$ Oe for NbGe and $H_\parallel\sim 700$ Oe for Nb) on the magnetization of the chosen ferromagnetic film.[30] The only strict condition for observation of the predicted effect is the shape of the domain structure—the domains should be directed along the direction of the transport current. In Co/Pd ferromagnet the pattern of domains is very complicated.[30]

This problem can probably be solved by using antiferromagnetic layers with the shape of stripes which are able to create the elongated in one direction domain due to so-called exchange bias effect or by using the ferromagnetic layers with steplike thickness, which also should favor the creation of the stripelike domains.

VI. CONCLUSIONS

In this paper the Meissner and vortex states of the ferromagnet/type-II superconductor bilayer were investigated when the ferromagnet has domain structure and perpendicular magnetic anisotropy. The system under consideration consists of two thin FM and SC films separated by finite distance a. We have calculated the values of the critical magnetization for the formation of two periodic vortex structures: (i) the chain of vortices (one vortice per domain) with alternating directions corresponding to the direction of the magnetization in the ferromagnetic domains and (ii) the mixed state of the SC (i.e., the structure with many vortices per domain) characterized by the average vortex density $n(x)$.

We derive the integrodifferential equation which determines the current and vortex distributions in the domain. Two assumptions were made in order to obtain this equation. First we suppose the periodic dependences of the current and vortex distributions on the coordinate x: $i(x)=i(x+2L)$, $n(x)=n(x+2L)$. A second assumption is that the current and vortex densities do not vary in the y direction so that we have an essentially one-dimensional problem. There are two characteristic limiting cases, $L<\lambda$ (the narrow-domain structure) and $L\gg\lambda$ (the wide-domain structure), for which the analytical solution of Eq. (10) can be obtained. In the latter the results are valid only if the distance a between the FM and SC films is large enough. Thus the analytical expression for Meissner current density [Eq. (17)] is in good agreement with the numerical solution of Eq. (10) for $a\geq 10\lambda$.

In ultrathin magnetic films the observed values of L vary in range, from 1 to 100 μm.[31,32] On the other hand the effective penetration depth $\lambda=\frac{\lambda_L^2}{d_s}$ essentially depends on the thickness d_s of the superconducting film and for ultrathin high T_c may reach the value of ~ 50 μm.[33] So both cases considered above may be realized in practice.

ACKNOWLEDGMENTS

This work was supported by the Russian Foundation for Basic Research and by the program of the Ministry of Science and Education of the Russian Federation. D.Y.V. acknowledges support from the Dynasty Foundation.

APPENDIX

Equation (20) for energy per vortex of the chain in the FM/SC bilayers with wide-domain structure does not include the interaction energy between the vortices E_{int} which is proportional to the small ratio $\lambda/L\ll 1$. To find the critical magnetization $m_1(a)$ we need to calculate this term. Consider the vortex located near the equilibrium position $x=L/2$ at $x=x_0$ in the domain $0\leq x\leq L$. Because the width of the domain L is much larger than the range of the vortex interaction in a thin SC film λ, we take into account only the interaction of the vortex with nearest vortices located at $x=2L-x_0$ and $x=-x_0$. As it is known the interaction energy between two vortices with different polarities is given by

$$E_{\text{int}}=-\frac{\Phi_0^2}{16\pi\lambda}\left[H_0\left(\frac{r}{2\lambda}\right)-Y_0\left(\frac{r}{2\lambda}\right)\right], \tag{A1}$$

where H_0 and Y_0 are Struve and Bessel functions and r is the distance between vortices. At distance $r\gg\lambda$ this yields

$$E_{\text{int}}=-\frac{\Phi_0^2}{4\pi^2 r}. \tag{A2}$$

Taking the above approach, it follows from Eq. (A2) that the interaction energy per vortex of the chain is

$$E_{\text{int}}(x_0)=-\frac{\Phi_0^2}{16\pi^2}\left(\frac{1}{L-x_0}+\frac{1}{x_0}\right) \tag{A3}$$

and, correspondingly,

$$E_s(x_0)=\frac{\Phi_0^2}{16\pi^2\lambda}\ln\frac{2\lambda}{\xi}+E_{\text{int}}(x_0). \tag{A4}$$

[1] I. F. Lyuksyutov and V. L. Pokrovsky, Adv. Phys. **54**, 67 (2005).
[2] D. J. Morgan and J. B. Ketterson, Phys. Rev. Lett. **80**, 3614 (1998).
[3] M. J. Van Bael, J. Bekaert, K. Temst, L. Van Look, V. V. Moshchalkov, Y. Bruynseraede, G. D. Howells, A. N. Grigorenko, S. J. Bending, and G. Borghs, Phys. Rev. Lett. **86**, 155 (2001).
[4] M. V. Miloševič and F. M. Peeters, Phys. Rev. B **69**, 104522 (2004).
[5] M. V. Miloševič and F. M. Peeters, Phys. Rev. B **68**, 024509 (2003).
[6] S. Erdin, Phys. Rev. B **72**, 014522 (2005).
[7] G. M. Maksimova, R. M. Ainbinder, and I. L. Maksimov, Phys. Rev. B **73**, 214515 (2006).
[8] M. V. Miloševič and F. M. Peeters, Phys. Rev. Lett. **93**, 267006 (2004).
[9] M. Lange, M. J. Van Bael, Y. Bruynseraede, and V. V. Moshchalkov, Phys. Rev. Lett. **90**, 197006 (2003).
[10] Yu. I. Bespyatykh and W. Wasilevski, Phys. Solid State **43**, 224 (2001).
[11] S. Erdin, I. F. Lyuksyutov, V. L. Pokrovsky, and V. M. Vinokur, Phys. Rev. Lett. **88**, 017001 (2001).
[12] R. Laiho, E. Lähderanta, E. B. Sonin, and K. B. Traito, Phys. Rev. B **67**, 144522 (2003).
[13] M. A. Kayali and V. L. Pokrovsky, Phys. Rev. B **69**, 132501

(2004).
[14] V. L. Pokrovsky and H. Wei, Phys. Rev. B **69**, 104530 (2004).
[15] S. Erdin, Phys. Rev. B **73**, 224506 (2006).
[16] A. I. Larkin and Yu. N. Ovchinnikov, Zh. Eksp. Teor. Fiz. **61**, 1221 (1971) [Sov. Phys. JETP **34**, 651 (1972)].
[17] K. K. Likharev, Radiophys. Quantum Electron. **14**, 909 (1971) [Izv. Vyssh. Uchebn. Zaved., Radiofiz. **14**, 714 (1971)].
[18] A. T. Dorsey, Phys. Rev. B **51**, 15329 (1995).
[19] I. S. Gradshteyn and I. M. Ryzhik, *Tables of Integrals, Series and Products* (Academic, New York, 1980).
[20] L. G. Aslamazov and S. V. Lempitskii, Zh. Eksp. Teor. Fiz. **84**, 2216 (1983) [Sov. Phys. JETP **57**, 1291 (1983)].
[21] D. Yu. Vodolazov, I. L. Maksimov, and E. H. Brandt, Europhys. Lett. **48**, 313 (1999).
[22] V. G. Kogan, Phys. Rev. B **49**, 15874 (1994); G. M. Maksimova, Phys. Solid State **40**, 1607 (1998).
[23] S. Erdin, A. F. Kayali, I. F. Lyuksyutov, and V. L. Pokrovsky, Phys. Rev. B **66**, 014414 (2002).
[24] M. V. Miloševič and F. M. Peeters, Phys. Rev. B **69**, 104522 (2004).
[25] I. L. Maksimov and G. M. Maksimova, JETP Lett. **65**, 423 (1997).
[26] M. Yu. Kupriyanov and K. K. Likharev, Fiz. Tverd. Tela (Leningrad) **16**, 2829 (1974) [Sov. Phys. Solid State **16**, 1835 (1975)].
[27] M. Benkraouda and J. R. Clem, Phys. Rev. B **58**, 15103 (1998).
[28] A. A. Elistratov, D. Y. Vodolazov, I. L. Maksimov, and J. R. Clem, Phys. Rev. B **66**, 220506(R) (2002).
[29] D. Babic, J. Bentner, C. Surgers, and C. Strunk, Phys. Rev. B **69**, 092510 (2004).
[30] W. Gillijns, A. Yu. Aladyshkin, M. Lange, M. J. Van Bael, and V. V. Moshchalkov, Phys. Rev. Lett. **95**, 227003 (2005).
[31] R. A. Allenspach and A. Bischof, Phys. Rev. Lett. **69**, 3385 (1992).
[32] O. Portmann, A. Vaterlaus, and D. Pescia, Nature (London) **422**, 701 (2003).
[33] F. Tafuri, J. R. Kirtley, D. Born, D. Stornaiuolo, P. G. Medaglia, P. Orgiani, G. Balestrino, and V. G. Kogan, Europhys. Lett. **73**, 948 (2006).